ELSEVIER

Ecological Modelling 86 (1996) 101–111

# Coupling a spatially-explicit forest gap model with a 3-D solar routine to simulate latitudinal effects

J.F. Weishampel [a,*], D.L. Urban [b]

[a] *Department of Biology, University of Central Florida, Orlando, FL 32816-2368, USA*
[b] *School of the Environment, Levine Science Research Center, Duke University, Durham, NC, 27708, USA*

Received 28 June 1994; accepted 14 December 1994

**Abstract**

A multi-scaled forest model (ZELIG) which spatially embeds patch-scale processes into a larger landscape was linked with a 3-D insolation routine to simulate the effects of latitudinal variation in solar radiation on the growth and spatial patterns of idealized early successional, shade-intolerant and late successional, shade-tolerant species. At the individual tree level, average tree height increased for the shade-intolerant species with decreasing latitude as steep angled direct-beam radiation more readily penetrated narrow canopy gaps. This yielded an increase in interspecific competition and intraspecific competition among shade-intolerant trees. Consequently, though stem density dropped, basal area of shade-intolerant species increased as growth increased with decreasing latitude. Conversely, basal area for the shade-tolerant species increased with increasing latitude as stem density increased as the proportion of diffuse radiation increased.

In terms of spatial pattern, the combined models produced non-random, anisotropic patterns which changed over the course of succession and were different for the shade-intolerant and tolerant species. However, differences in spatial patterns for the tropical, temperate, and boreal solar regimes were inexplicable. Shade-tolerant species consistently exhibited negative autocorrelation on adjacent grid cells (10–20 m away) during early successional stages and later stages after species replacement. Auto-correlation of shade-intolerant species shifted from negative to positive at this scale as its role changed from canopy dominant to gap colonizer. At scales > 20 m, whether or not a specific direction/distance autocorrelation value was positive or negative and significant or not significant was highly variable for both species and was attributed to stochastic properties (i.e., birth and mortality) of the model.

*Keywords:* Forest ecosystems; Latitude; Shading; Solar radiation; Spatial patterns

## 1. Introduction

Latitudinal variation in solar radiation not only contributes to variation in forest structure (e.g., strata; Smith, 1973; Terborgh, 1985), tree architecture (e.g., branching angles and crown shape;

* Corresponding author. Present address: Department of Biology, P.O. Box 2368, University of Central Florida, Orlando, FL 32816-2368, USA.


*SSDI* 0304-3800(94)00201-0

Kuuluvainen, 1992), and leaf attributes (e.g., orientation, shape, size, evergreenness; Sprugel, 1989), but also contributes to the patterns and processes of forest dynamics. Average solar altitude angles decrease with increasing latitude, thereby increasing the importance of diffuse radiation and the average shadow length which is thought to augment the effective canopy gap size (Prentice and Leemans, 1990). Thus, natural regenerative disturbances required for gap-phase replacement range from single treefall gaps in the tropics ($> 20$ m$^2$; Brokaw, 1982) to multiple-treefall disturbances such as those caused by forest fires in the boreal zone (i.e., $> 1$ km$^2$).

The resulting effect of variations of gap size on species establishment with respect to shade-tolerance and successional replacement patterns have been observed (Brokaw, 1985; Spies and Franklin, 1989) and modeled without consideration of latitudinal effects (Urban et al., 1991). As gap size increased, so did the richness of shade-intolerant species. When the effects of solar geometry were included, a north–south transect version of a gap model generated a less dense understory at high latitudes compared to the low latitude scenario. The mature, undisturbed boreal-zone forest tended to support only shade-tolerant species, whereas the mature tropical-zone forest with substantially more steep-angled, direct beam radiation allowed shade-intolerant species to persist (Urban et al., 1991).

However, solar effects are not a 2-D (i.e., solar altitude angle and direction), north–south phenomenon. The spatial distribution of light around a tree and forest gap (Canham et al., 1990) in 3-D also varies with the solar geometry, (i.e., season, latitude, slope, and aspect). Combining solar radiation (Bonan, 1989; Nikolov and Zeller, 1992) /shading (Kuuluvainen and Pukkala, 1987; Granberg, 1988) algorithms with spatially-explicit forest models (Smith and Urban, 1988; Busing, 1991; Pacala et al., 1993) allows for the exploration of light-mediated spatial patterns across a forested landscape. This study merged a 3-D insolation routine with a gap model, ZELIG (Urban, 1990), forming a 3-D gap model with interactive plot-to-plot shading, to test the sensitivity of successional growth and spatial patterning of shade-tolerant and intolerant species to solar latitudinal effects.

## 2. Methods

### 2.1. Computation of the 3-D solar regimes

The methodology of Bonan (1989) was adapted to derive the average yearly solar altitude angle ($\theta$) and the average proportion of direct beam radiation ($\phi_b$) impinging on each side of a ZELIG grid cell ($10 \times 10$ m) divided into 45° angles (i.e., N, NE, E, SE, S, SW, W, NW) over the course of a growing season. This was done for three latitudes, 58.37°N, 36.08°N, and 17.52°N, respectively representing boreal, temperate, and tropical zones. Their growing season lengths were estimated to be, respectively, from April through October, March through November, and January through December. The solar azimuth angle for a given latitude ($\lambda$) was determined over the course of the day which represents the daily monthly average of extraterrestrial radiation (Klein, 1977) at minute intervals. This was done by calculating the solar declination ($\delta$) and the sunrise/sunset hour angle from solar noon (0°) and multiplying by 8 to give the day length in minutes. Then for each minute ($i$) representing successive 0.25° angles ($\omega$) between the sunrise and sunset angles (i.e., when $\theta_i$ was $> 0°$):

$$\theta_i = \sin^{-1}[\sin(\lambda)\sin(\delta) + \cos(\lambda)\cos(\delta)\cos(\omega)].$$

For each minute, $\phi_{b_i}$ was calculated from estimates of extraterrestrial solar radiation ($H_0$) received on a horizontal surface (Klein, 1977) corrected for atmospheric (i.e., scattering and absorbing) effects. Bonan (1989) developed an equation for the North American boreal zone to relate monthly terrestrial solar radiation ($H$) received on a horizontal plane at the earth's surface (cal · cm$^{-2}$ · day$^{-1}$) to monthly cloudiness in tenths of sky ($c$). Likewise, we used meteorological data from eastern United States (Bennet, 1965; Court, 1974) and Central America (Portig, 1976) to derive linear regressions to account for the monthly attenuation of solar radiation through

the atmosphere in the temperate (for 24 sites over 12 months, $R^2 = 0.980$):

$$H = -52.192 + 0.818\,H_0 - 0.035\,H_0\,(c/10);$$

and tropical zones (for 1 site over 12 months, $R^2 = 0.978$):

$$H = 252.7 + 0.695\,H_0 - 0.695\,H_0\,(c/10).$$

For the simulations, cloudiness data from Juneau (Alaska), Greensboro (North Carolina), and Belize City (Belize) representing the three latitudinal regions were used. The fraction of terrestrial to extraterrestrial radiation ($H/H_0$) was used to compute the ratio of diffuse ($\phi_{d_i}$) to terrestrial radiation (Keith and Kreider, 1978; Bonan, 1989) for each minute:

$$\phi_{d_i}/H = 1.0045 + 0.0435(H/H_0) - 3.5227(H/H_0)^2 + 2.6313(H/H_0)^3.$$

If $H/H_0 > 0.75$, $\phi_{d_i}/H = 0.166$. Thus, $\phi_{b_i} = H - \phi_{d_i}$. From the total minutes spent in each directional 45° zone, $\theta$ and $\phi_b$ were calculated.

The latitudinal differences from these procedures are shown in Fig. 1. The average shadow lengths for a 20-m-tall tree (i.e., $20 \cdot \tan^{-1}\theta$) for the three latitudes vary slightly in the W, NW, N, NE, and E directions with the shadow lengths being longer in the E and W directions. Because the effects of slope and aspect were not introduced, shadows were always symmetrical in the E–W direction. As expected, the shadows in the northern direction increased with latitude from 12 to 14 to 23 m. The high latitude zone yielded long shadows in the SW and SE directions representing flat summer sunrise and sunset angles, respectively, but, the percent of growing season time when this occurred or the proportion of $\phi_b$ contributing to this phenomenon was small. Shadows at the mid latitude zone occurred only north of the N–S division, whereas shadows from the low latitude zone were nearly symmetrical around the N–S division. Because all the sites were from the northern hemisphere, the proportion of $\phi_b$ was greatest in the N direction. The mid latitude zone, without any southerly shadows, represents the most N–S asymmetrical distribution of $\phi_b$. At 0° latitude, there would be complete (i.e., N–S and E–W) symmetry. The proportion of diffuse radiation ($\phi_d$) was greatest at the high latitude, substantially decreasing towards the mid and low latitudes.

### 2.2. Development of the 3-D ZELIG model

The 3-D ZELIG model, like the original version (Smith and Urban, 1988) operates on a square grid of gap-sized (10 × 10 m) cells. However, unlike the original version, this version explicitly models the light regime in space. The 3-D version essentially follows the same interactive solar routine found in the transect version (Urban et al., 1991; Weishampel et al., 1992), however, instead of there being a single S–N transect, there are four transects (i.e., eight directions) representing the four cardinal directions and their midpoints. Light ($\phi_b$ and $\phi_d$) attenuates in an negative-exponential fashion through the canopy to a cell and height position on the grid. Tree height is derived from the polynomial function of diameter from Botkin et al. (1972). Diameter growth is modified by available light. Crown depth estimation follows Leemans and Prentice (1987) and is a function of tree height and shading from higher leaves.

For each direction where $\phi_b > 0$, $\phi_b$ passes through the canopy at the predetermined $\theta$. Whereas $\phi_d$ is sampled in six directions from an isotropic sky (see Urban and Shugart, 1992) from each directional transect and the vertical direction (i.e., a total of 25 samples). Light penetration from the diagonal directions (i.e., NE–SW, SW–NE, SE–NW, and NW–SE) is corrected for the increased distance that it must travel through the canopy. Thus, a 20-m-tall tree in the northern latitude scenario which casts a shadow 329 m long in the SE or SW direction could feasibly influence a tree 23 diagonal plots away (Fig. 2). But given the low level of $\phi_b$ in this direction it is unlikely that light would be able to penetrate canopies a few diagonal plots away. Upon reaching the edge of the grid, the shadow "wraps around" offset by one cell to ensure that a tree does not shade itself from the opposite direction.

Fifty grids of 20 × 20 plots were simulated for

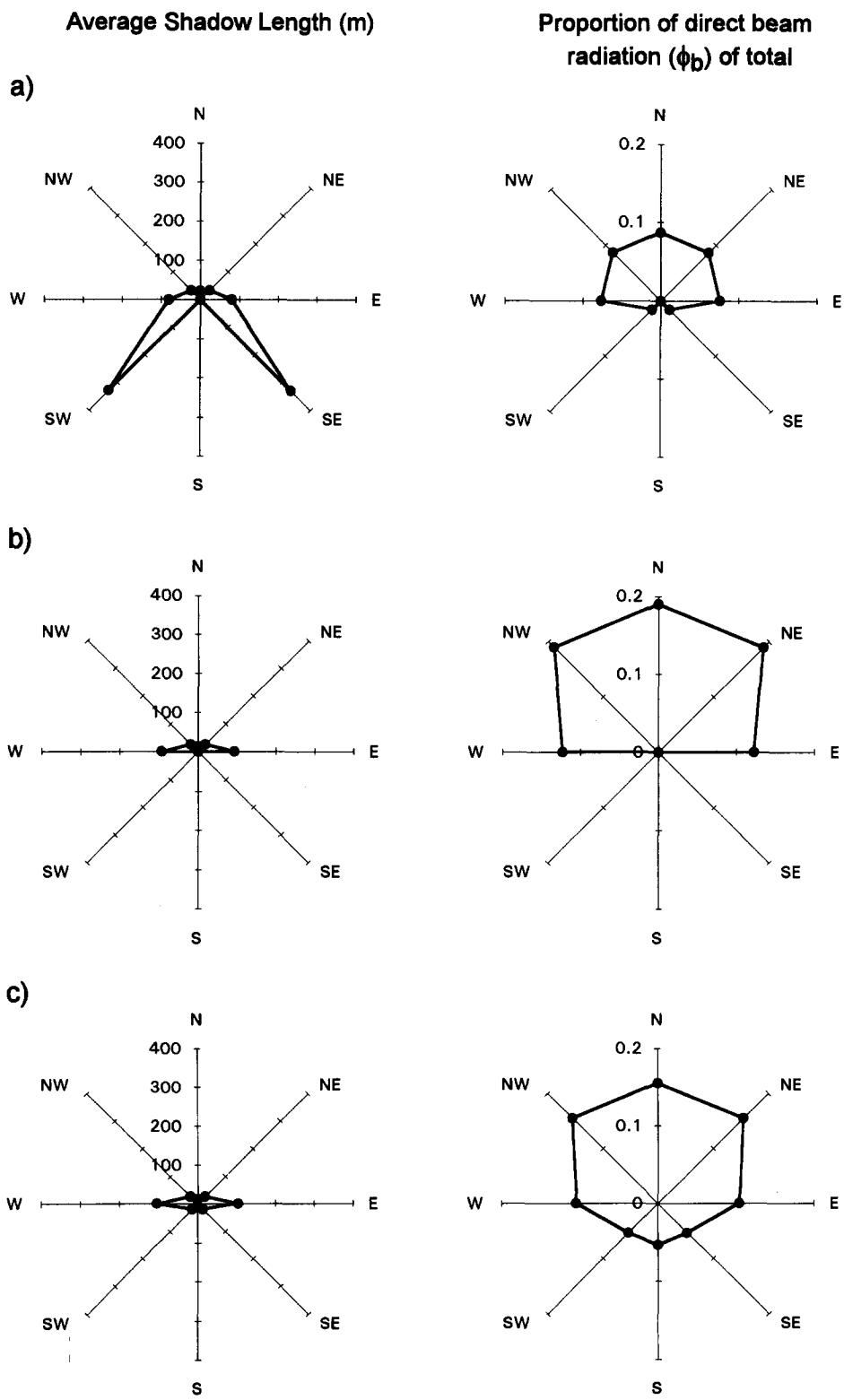
Average Shadow Length (m)
Proportion of direct beam radiation ($\phi_b$) of total
a)
b)
c)
N
NE
E
SE
S
SW
W
NW
400
300
200
100
0.2
0.1
0

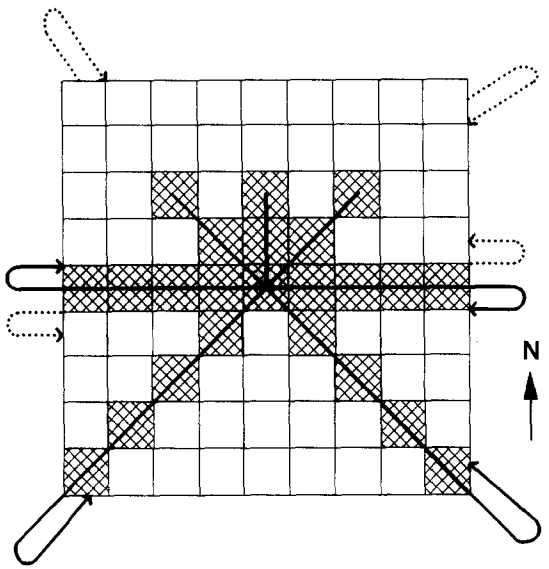


Fig. 2. Schematic of a 9×9 ZELIG grid detailing the potential shading zone of influence of a 20-m-tall tree in the high latitude environment. Arrows beyond the grid indicate a shadow longer than the grid which require "wrapping around" to minimize edge effects.

each latitudinal scenario for 400 years. Species parameters representing a shade-intolerant (SPPI) and a shade-tolerant (SPPT) species similar to those used by Huston and Smith (1987) to model patterns of two-species competition were selected to model successional replacement with the 3-D ZELIG (Table 1). Because the emphasis was on light-mediated competition, the soil moisture, temperature, and nutrient responses found in other versions of the model were excluded from these runs.

### 2.3. Directional spatial pattern analysis

Spatial autocorrelation quantifies the geographic dependence of spatially distributed variables. Because solar interaction among ZELIG cells is anisotropic and varies with latitude, it was of interest to examine the directional variation of

Table 1
Parameters for simulated species

| Species | $A_{max}$ | $D_{max}$ | $H_{max}$ | GR | L | S |
|---|---|---|---|---|---|---|
| SPPI | 175 | 100 | 2500 | 150 | 5 | 5 |
| SPPT | 350 | 200 | 5000 | 100 | 1 | 1 |

$A_{max}$ = maximum age (yr); $D_{max}$ = maximum diameter at breast height (cm); $H_{max}$ = maximum height (cm); GR = growth rate (dimensionless); L = shade tolerance rank (1 = very tolerant); S = sapling establishment rank (SPPI has a 5-fold advantage over SPPT).

auto-correlation over the gridded forest stands. This was achieved by using 2-D correlograms (Oden and Sokal, 1986; Jacquez, 1991). This technique and similar techniques (e.g., 2-D spectral analysis and directional variograms) have been used by forest ecologists to detect 2-D spatial pattern in the distribution of trees (Ford and Renshaw, 1984; Legendre and Fortin, 1989; Weishampel et al., 1994) and forest attributes such as canopy roughness (Ford, 1976), across a range of scales. Similar techniques have also been used to detect the presence of spatial competition for light by plants in greenhouse experiments (Ford, 1975; Ford and Diggle, 1981; Renshaw, 1984).

Moran's $I$ (Griffith, 1988) was chosen as the measure of autocorrelation. Assuming isotropy for a 2-D plane comprised of $n$ observations of $x$:

$$I = \frac{\left(n / \sum_{i=1}^{n}\sum_{j=1}^{n} w_{ij}\right)\sum_{i=1}^{n}\sum_{j=1}^{n} w_{ij}(x_i-\bar{x})(x_j-\bar{x})}{\sum_{i=1}^{n}(x_i-\bar{x})^2}$$

The weighting term $w_{ij}$ denotes the connection between observations $i$ and $j$ across a range of lag distances. If the distance between $x_i$ and $x_j$ equals the appropriate lag distance, $w_{ij} = 1$; if not, $w_{ij} = 0$. Moran's $I$ values, being weighted product-moment correlation coefficients, range between $-1$ and $+1$. Positive and negative values signify positive and negative autocorrelations.

Fig. 1. The average shadow length around a 20-m-tall tree and the corresponding proportion of direct beam radiation associated with the eight primary compass directions over the course of a growing season for (a) high (i.e., 58.37°N), (b) mid (i.e., 36.08°N), and (c) low (i.e., 17.52°N) latitude scenarios. Proportions of diffuse radiation ($\phi_d$) were 0.55, 0.19, and 0.17, respectively.

Extending Moran's $I$ to yield directional correlograms entails making comparisons only between observations at a certain direction and distance away from the initial observation. For this exercise, the basal area of SPPI and SPPT from each grid cell were the observed variables. Because comparisons in a direction equal comparisons 180° away, the upper and lower halves of a 2-D correlogram are symmetrical. For the $20 \times 20$ grids, five annuli (i.e., circular lag distances) were used. The innermost annulus represents distances between 10 and $< 20$ m (1 and $< 2$ grid cell units) away. The radiating annuli represent distances from 20 to $< 40$ m, 40 to $< 60$ m, 60 to $< 80$ m and 80 to $< 100$ m. With each annulus the possible directions analyzed increased from one direction in the innermost annulus to nine directions in the outermost annulus. Because the range for each annulus always exceeded one grid cell, the number of comparisons for each distance/direction class was always $> 1000$. Significance ($P < 0.05$) of the autocorrelation coefficient for a given distance/direction class was gauged by calculating Moran's $I$ under normalized and randomized assumptions (Jacquez, 1991).

## 3. Results and discussion

### 3.1. Latitudinal effects on shade-tolerant / intolerant growth

Differences among the scenarios in terms of the timing of species replacement and the magnitude of species basal area throughout succession are shown in Fig. 3. Generally, the lower latitude scenarios showed a small delay in species replacement and higher levels of SPPI basal area after SPPT dominated the stand. Prior to species replacement (i.e., $\approx 100$ yrs) the magnitude of SPPT basal area became progressively higher with increasing latitude. The fact that differences in the persistence of the shade-intolerant species were not as profound as with the Urban et al. (1991) transect study may reflect the reduced importance of steep-angled southerly light, as direct beam radiation was divided among eight directional faces (i.e., for the tropical scenario) instead of a single south–north one.

Three time periods (i.e., 100, 200, and 400 yr) were chosen for further analysis. They represent two dynamic periods, during and $\approx 100$ yrs after species replacement, and a relative steady state of SPPT dominance. At the individual tree level for a $20 \times 20$ grid run (Fig. 4), there was a progressive decrease in average SPPI tree height with time. SPPT exhibited a peak in average tree height at 200 yr. SPPI per plot stem density was highest at 100 yr and lowest at 200 yr. SPPT stem density was highest at 100 yr. Though latitudinal differences in stand-level structure (i.e., basal area) were negligible for SPPI, they were manifest at the individual tree level. Significant latitudinal differences in height, determined by a $t$-test, existed only with the shade-intolerant species for these time periods. At 100 yr, average SPPI height at the high latitude scenario was less than the mid and low latitudinal scenarios. As a result of this increased intraspecific competition, SPPI density significantly decreased with decreasing latitude. At 400 yr, SPPI height again increased with decreasing latitude. The recruitment of SPPI at 100 and 400 yrs occurs in relatively narrow ($10 \times 10$ m) gaps as result of canopy dominant SPPI and SPPT trees, respectively. At 200 yr, tree mortality is more a function of understory sup-

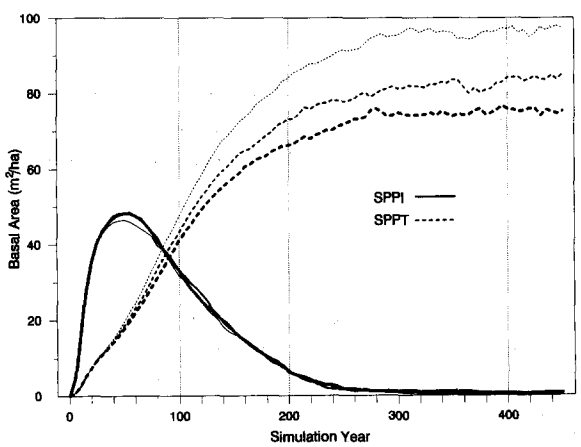


Fig. 3. Temporal trace of basal area of the early successional shade-intolerant (i.e., SPPI) and the late successional shade-tolerant (i.e., SPPT) species showing species replacement for the three latitude scenarios. The thick, medium, and thin lines respectively represent the tropical-, temperate-, and boreal-zone simulations.

pression. The increase in shade-intolerant tree height with decreasing latitude reflects the deeper penetration of steep angled direct beam radiation into a gap. This vertical component of radiation also played a significant role in the high latitude scenarios; however, it was comprised primarily of diffuse radiation ($\phi_d = 0.55$). In these simulations, the vertical component of diffuse radiation comprised 2.2% and 0.3% of the total radiation for the high and low latitude scenarios, respectively. Though insufficient to produce differences in growth rate of the species, this increase in vertical light permitted a general increase in the abundance of shade-tolerant stems. Increasing SPPT stem density with latitude, to a certain extent, may reflect a decrease in interspecific competition.

### 3.2. Successional spatial patterns of shade-tolerant / intolerant species

Individual landscapes from a latitudinal scenario varied greatly in terms of where significant autocorrelation and positive and negative $I$ values occurred. This was a result of the underlying stochastic processes (i.e., birth and death) in the gap model contributing to the shifting mosaic forest landscape. Although to derive $I$ values for each direction/ distance class for a given scenario over 1000 comparisons among the 400 grid cells were made, stochastic processes acted to the benefit or detriment of trees on a given plot possibly causing a cascade of feedbacks, thereby altering the entire landscape. Thus, to better describe the influence of latitudinal regimes on the directional spatial patterns of species, $I$ values from the 50 landscape simulations were averaged.

Though latitudinal differences of basal area when taken out of their spatial context (e.g., Fig. 3) were evident, less pronounced differences in spatial patterns occurred over the course of the simulations. However, unlike a previous modeling study (Weishampel et al., 1992) which found structural attributes (i.e., biomass, leaf area, and maximum tree height) of Pacific Northwest forests to be randomly distributed along a 5-km transect of $10 \times 10$ m plots, different, anisotropic, nonrandom, 2-D spatial patterns existed for the basal areas of both the shade-tolerant and shade-intolerant species for the three latitude scenarios (Figs. 5–7). These patterns of directional autocor-

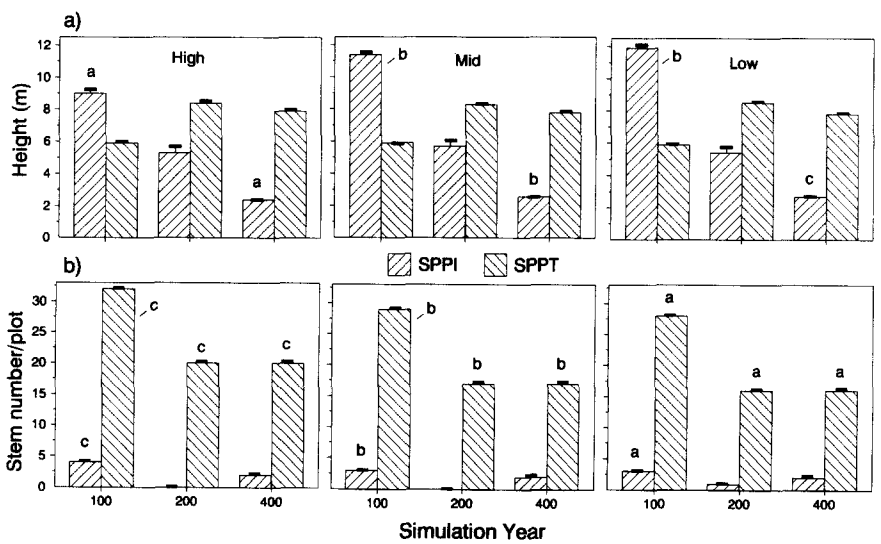


Fig. 4. Average (a) tree height for each tree and (b) per plot density from a $20 \times 20$ plot simulation for the latitudinal scenarios. Extensions above the bars represent standard error. Bars without letters or possessing similar letters indicate non significant differences among latitude scenarios for a given time period, otherwise a < b < c ($P < 0.05$).

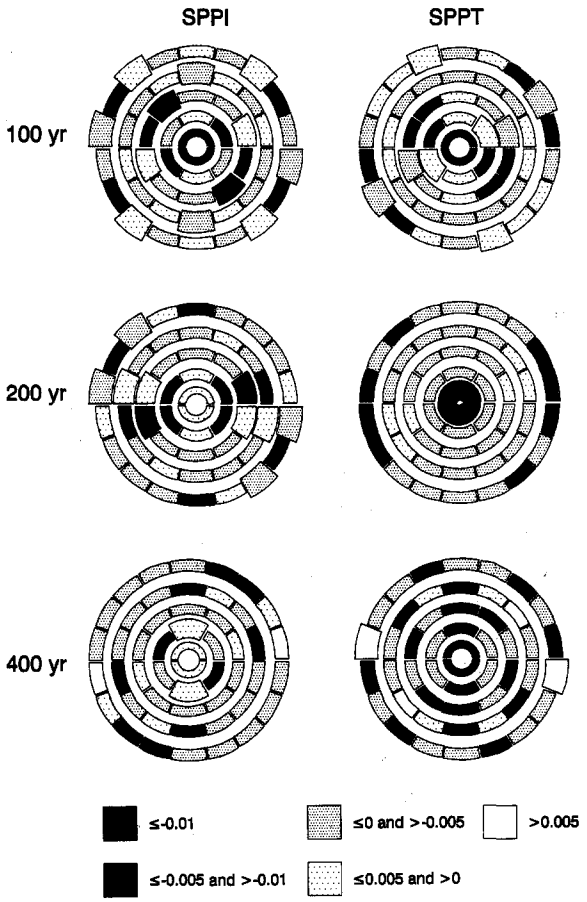


Fig. 5. 2-D correlograms for SPPI and SPPT at 100, 200, and 400 yr for the high latitude (i.e., 58.37°) scenario. Shading indicates the average Moran's $I$ value for the 50 simulations for each direction/distance class detailed in the text. Larger boxes within an annulus represent direction/distance classes where there were $\geq 5$ significant ($P < 0.05$) $I$ values.

relation changed over the course of succession for each species. However, the scale of autocorrelation did not increase with increasing latitude to reflect the belief that between-tree spacing and effective gap size increases with latitude as a function of increasing shadow length. Moreover, the asymmetrical patterns of shading did not correspond to interpretable directional patterns. A finer temporal resolution (e.g., $\approx$ 10 yrs) may be necessary to track directional changes which may also be diluted by averaging the simulated landscapes. Because the primary shading from $\phi_b$ (i.e., in the N, NE, and NW directions) from 20-m-tall trees cast shadows $< 30$ m (Fig. 1), a finer spatial resolution e.g., 0.5-m resolution in SPACE (Busing, 1991) may be necessary to capture directional or scale-related latitudinal variation. This is especially true since trees were considerably shorter on average during the course of the simulations (Fig. 4).

Disregarding directional variation (Fig. 8), the absolute value of autocorrelation was highest within the innermost annulus distance (i.e., 10–< 20 m). Because cell-to-cell interaction was driven by capturing light and casting shade, there were

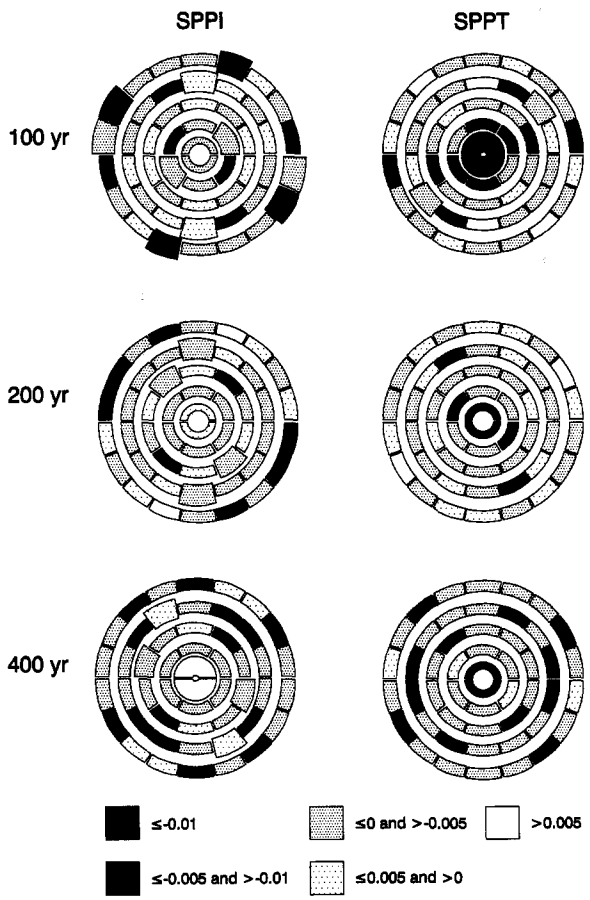


Fig. 6. 2-D correlograms for SPPI and SPPT at 100, 200, and 400 yr for the mid latitude (i.e., 36.08°) scenario. Shading indicates the average Moran's $I$ value for the 50 simulations for each direction/distance class detailed in the text. Larger boxes within an annulus represent direction/distance classes where there were $\geq 5$ significant ($P < 0.05$) $I$ values.

no positive feedbacks among grid cells which would generate positive correlations. Thus, average $I$ values tended to be negative across the majority of distance classes and positive correlations occurred only in the absence of or with a reduction of the negative competitive feedback.

As found with tree height, it was expected that the different light regimes should have a more dramatic effect on the autocorrelative properties of the shade-sensitive species than those from the shade-insensitive species. This was not the situation for the sampled time periods as SPPI revealed lower absolute autocorrelation values than SPPT. The two species-types revealed different spatial autocorrelative patterns with succession at scales between 10 and < 20 m. At 100 yr, for all latitudinal scenarios, SPPI exhibited negative autocorrelations. By 200 yr, these $I$ values increased to $\approx 0$. By 400 yr, these values were all positive. This positive association of shade-intolerant species at 400 yr may reflect the presence of a gap in the SPPT dominated canopy permitting lateral light to penetrate adjacent cells and the subsequent growth of SPPI. For SPPT, spatial auto-correlation in the innermost annulus was negative for all the sampled time periods with the majority having five or more significant $I$ values. The 10–< 20 m region may represent a significant scale of pattern for intraspecific competition which was relatively unchanged during the sampled periods of succession for SPPT.

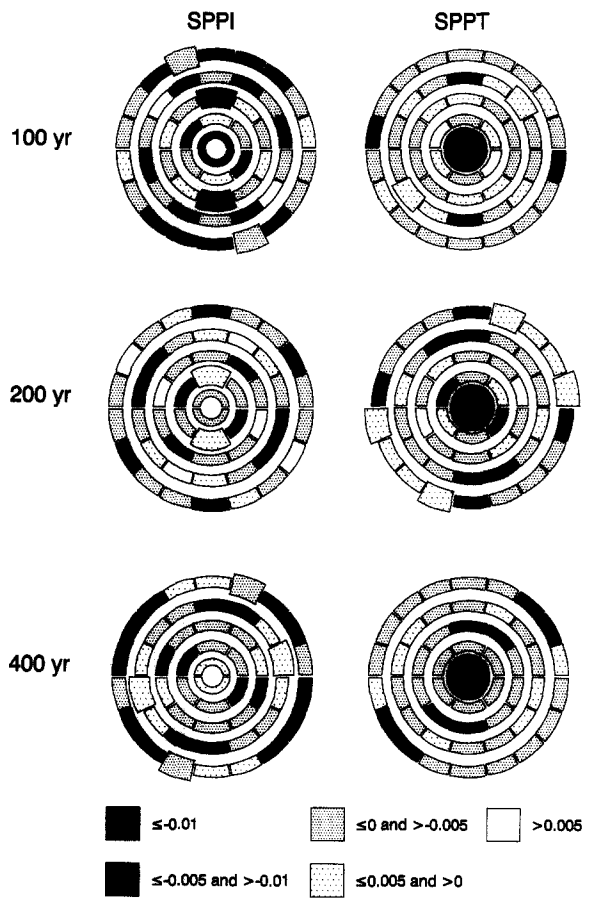


Fig. 7. 2-D correlograms for SPPI and SPPT at 100, 200, and 400 yr for the low latitude (i.e., 17.52°) scenario. Shading indicates the average Moran's $I$ value for the 50 simulations for each direction/distance class detailed in the text. Larger boxes within an annulus represent direction/distance classes where there were $\geq 5$ significant ($P < 0.05$) $I$ values.

Although differences between the autocorrelative patterns of SPPI and SPPT existed, 100 and 200 yr represent periods of decendancy for SPPI and periods of ascendancy for SPPT while 400 yr represents a period of SPPT dominance. With the reduction of SPPI density, there was also a decrease in intraspecific competition while SPPT density and intraspecific competition was increasing. A more appropriate comparison may be at 25 or 50 yr for SPPI when its basal area is rising or peaking, respectively.

The inability of the model to produce latitudinal differences in the spatial distribution of shade-tolerant and intolerant species may not only be scale related. Though this version of ZELIG, unlike traditional gap models, incorporated crown volume, as modeled by Leemans and Prentice (1987), evolutionary adaptations of trees such as crown shape (Terborgh, 1985; Kuuluvainen and Pukkala, 1989) and leaf shape (Sprugel, 1989) possibly adapted to differences in latitudinal light (Kuuluvainen, 1992) were not considered. If latitudinal differences in light capturing mechanisms were incorporated by simulating different structural types, results would undoubtedly differ. However, to fully model the benefits of certain adaptations (i.e., crown shape or vertically oriented leaves), solar radiation impinging on non horizontal surfaces (van der Hage, 1993) would need to be considered and the assumption

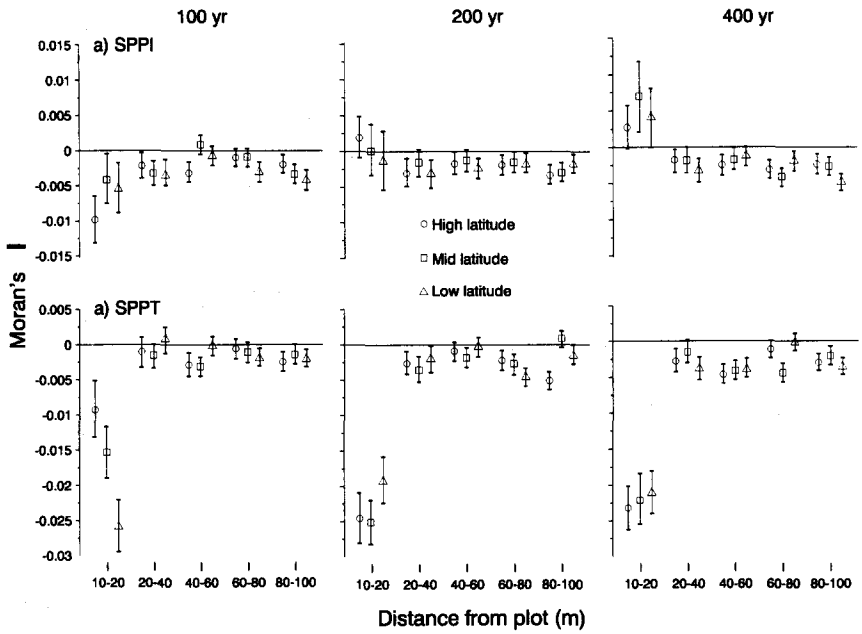


Fig. 8. Average Moran's $I$ values as a function of distance from a given plot for (a) SPPI and (b) SPPT at 100, 200, and 400 yr for the different latitudinal scenarios. The bars above and below the marker indicate ± standard error for the averaged direction classes over the 50 simulations.

of horizontal homogeneity at the plot level would need to be abandoned in favor of a finer scale, tree-to-tree modeling approach (e.g., Busing, 1991; Pacala et al., 1993). To match the level of structural detail, the solar routine may need to be altered to include phenomena such as sunflecks which have been estimated to contribute 37–68% of photosynthetically active radiation (PAR) for tropical forests and species-specific shading differences (Canham et al., 1990).

## Acknowledgements

We wish to thank Bruce Hayden, Hank Shugart, Tom Smith, Henry Wilbur and two anonymous reviewers for comments on earlier drafts of this paper. This work was supported in part by a National Aeronautics Space Administration Graduate Fellowship in Global Change Research and a National Research Council research associateship.

## References

Bennet, I., 1965. Monthly maps of mean daily insolation for the United States. Solar Energy, 9: 145–158.

Bonan, G.B., 1989. A computer model of the solar radiation, soil moisture, and soil thermal regimes in boreal forests. Ecol. Model., 45: 275–306.

Botkin, D.B., Janak, J.F. and Wallis, J.R., 1972. Some ecological consequences of a computer model of forest growth. J. Ecol., 60: 849–873.

Brokaw, N.V.L., 1982. The definition of treefall gap and its effect on measures of forest dynamics. Biotropica, 14: 158–160.

Brokaw, N.V.L., 1985. Gap-phase regeneration in a tropical forest. Ecology, 66: 682–687.

Busing, R.T., 1991. A spatial model of forest dynamics. Vegetatio, 92: 167–179.

Canham, C.D., Denslow, J.S., Platt, W.J., Runkle, J.R., Spies, T.A. and White, P.S., 1990. Light regimes beneath closed canopies and tree-fall gaps in temperate and tropical forests. Can. J. For. Res., 20: 620–631.

Court, A., 1974. The climate of the conterminous United States. In: R.A. Bryson and F.K. Hare (Editors), Climates of North America. World Survey of Climatology 11. Elsevier, Amsterdam, pp. 193–266.

Ford, E.D., 1975. Competition and stand structure in some even-aged monocultures. J. Ecol., 63: 311–333.

Ford, E.D., 1976. The canopy of a Scots pine forest: description of a surface of complex roughness. Agric. Meteorol., 17: 9–32.

Ford, E.D. and Diggle, P.J. 1981. Competition for light in a plant monoculture modelled as a spatial stochastic process. Ann. Bot., 48: 481–500.

Ford, E.D. and Renshaw, E., 1984. The interpretation of process from pattern using two-dimensional spectral analysis: modelling single species patterns in vegetation. Vegetatio, 56: 113–123.

Granberg, H.D., 1988. A forest shading model using bitmapped graphics. Agric. For. Meteorol., 43: 225–234.

Griffith, D.A., 1988. Advanced Spatial Statistics. Kluwer, Boston, MA, 273 pp.

Huston, M.L. and Smith, T.M., 1987. Plant succession: life history and competition. Am. Nat., 130: 168–198.

Jacquez, G.M., 1991. C2D: Spatial Autocorrelation in Two Dimensions. Exeter Publishing, Setauket, New York, 52 pp.

Keith, F. and Kreider, J.F., 1978. Principles of Solar Engineering. Hemisphere, Washington, DC, 778 pp.

Klein, S.A., 1977. Calculation of monthly average insolation on tilted surfaces. Solar Energy, 19: 325–329.

Kuuluvainen, T., 1992. Tree architectures adapted to efficient light utilization: is there a basis for latitudinal gradients? Oikos, 65: 275–284.

Kuuluvainen, T. and Pukkala, T., 1987. Effect of crown shape and tree distribution on the spatial distribution of shade. Agric. For. Meteorol., 40: 215–231.

Kuuluvainen, T. and Pukkala, T., 1989. Simulation of within-tree and between-tree shading of direct radiation in a forest canopy: Effect of crown shape and sun elevation. Ecol. Model., 49: 89–100.

Leemans, R. and Prentice, I.C., 1987. Description and simulation of tree-layer composition and size distributions in a primaeval *Picea–Pinus* forest. Vegetatio, 69: 147–156.

Legendre, P. and Fortin, M., 1989. Spatial pattern and ecological analysis. Vegetatio, 80: 107–138.

Nikolov, N.T. and Zeller, K.F., 1992. A solar radiation algorithm for ecosystem dynamic models. Ecol. Model., 61: 149–168.

Oden, N.L. and Sokal, R.R., 1986. Directional autocorrelation: An extension of spatial correlograms in two dimensions. Syst. Zool., 35: 608–617.

Pacala, S.W., Canham, C.D. and Silander, J.A., 1993. Forest models defined by field measurements: I. the design of a northeastern forest simulator. Can. J. For. Res., 23: 1980–1988.

Portig, W.H., 1976. The climate of Central America. In: W. Schwerdtfeger (Editor), Climates of Central and South America. World Survey of Climatology 12. Elsevier, Amsterdam, pp. 405–478.

Prentice, I.C. and Leemans, R., 1990. Pattern and process and the dynamics of forest structure: a simulation approach. J. Ecol., 78: 340–355.

Renshaw, E., 1984. Competition experiments for light in a plant monoculture: an analysis based on two-dimensional spectra. Biometrics, 40: 717–728.

Smith, A.P., 1973. Stratification of temperate and tropical forests. Am. Nat., 107: 671–683.

Smith, T.M. and Urban, D.L., 1988. Scale and resolution of forest structural pattern. Vegetatio, 74: 143–150.

Spies, T.A. and Franklin, J.F., 1989. Gap characteristics and vegetation response inconiferous forests of the Pacific Northwest. Ecology, 70: 543–545.

Sprugel, D.G., 1989. The relationship of evergreenness, crown architecture, and leaf size. Am. Nat., 133: 465–479.

Terborgh, J., 1985. The vertical component of plant species diversity in temperate and tropical forests. Am. Nat., 126: 760–776.

Urban, D.L., 1990. A versatile model to simulate forest pattern: a user's guide to ZELIG version 1.0. Department of Environmental Sciences, University of Virginia, Charlottesville, VA, 108 pp.

Urban, D.L. and Shugart, H.H., 1992. Individual-based models of forest succession. In: D.C. Glenn-Lewin, R.K. Peet and T.T. Veblen (Editors), Plant Succession: Theory and Prediction. Chapman and Hall, London, pp. 249–286.

Urban, D.L., Bonan, G.B., Smith, T.M. and Shugart, H.H., 1991. Spatial applications of gap models. For. Ecol. Manage., 42: 95–110.

van der Hage, J.C.H. 1993. The horizontal component of solar radiation. Agric. For. Meteorol., 67: 79–93.

Weishampel, J.F., Urban, D.L., Shugart, H.H. and Smith, J.B., 1992. Semivariograms from a forest transect gap model compared with remotely sensed data. J. Veg. Sci., 3: 521–526.

Weishampel, J.F., Sun, G., Ranson, K.J., LeJeune, K.D. and Shugart, H.H., 1994. Forest textural properties from simulated microwave backscatter: the influence of spatial resolution. Rem. Sens. Environ., 47: 120–131.